JOURNAL OF AIRCRAFT
Vol. 31, No. 5, Sept.–Oct. 1994

Aerodynamic Sensitivity Coefficients Using the Three-Dimensional Full Potential Equation

Hesham M. El-banna* and Leland A. Carlson†
Texas A&M University, College Station, Texas 77843

The quasianalytical (QA) approach is applied to the three-dimensional full potential equation to compute wing aerodynamic sensitivity coefficients in the transonic regime. Symbolic manipulation is used and is crucial in reducing the effort associated with obtaining sensitivity equations, and the large sensitivity system is solved using sparse solver routines such as the iterative conjugate gradient method. The results obtained are almost identical to those obtained by the finite difference (FD) approach and indicate that obtaining the sensitivity derivatives using the QA approach is more efficient than computing the derivatives by the FD method, especially as the number of design variables increases. It is concluded that the QA method is an efficient and accurate approach for obtaining transonic aerodynamic sensitivity coefficients in three dimensions.

Nomenclature

C = maximum camber in fraction of chord
CL = wing lift coefficient
Cl = section lift coefficient
Cp = pressure coefficient
$c(y)$ = chord function
L = chordwise location of maximum camber in fraction of chord
M = local Mach number
M_c = cutoff Mach number $0.94 \leq M_c \leq 1.0$
M_∞ = freestream Mach number
P_∞ = freestream pressure, nondimensionalized by $[2\gamma/(\gamma + 1)]P_0$
q_∞ = freestream velocity, nondimensionalized by V^*
T = maximum thickness in fraction of chord
$T_{1..4}$ = twist angles at 0, 20, 60, and 100% semispan
U, V, W = contravariant velocity components
V^* = critical speed
X, Y, Z = computational coordinates
$\boldsymbol{XD}$ = vector of design variables
XL_T, $XLET$ = x coordinate of leading edge of wingtip
XT_T, $XTET$ = x coordinate of trailing edge of wingtip
x, y, z = physical grid system
$xle(y)$ = leading-edge function
Y_T, $SSPAN$ = y coordinate of wingtip
α = angle of attack
Γ = circulation
γ = ratio of specific heats
$\bar{\delta}(\ )$ = first-order backward difference operator
ν = switching function
ρ = density, nondimensionalized ρ_0
$\tilde{\rho}$ = retarded density
ρ_0 = stagnation density
ρ_∞ = freestream density, nondimensionalized by ρ_0
Φ = full potential function
ϕ = reduced potential function

Introduction

TO design transonic vehicles using optimization techniques requires aerodynamic sensitivity coefficients, which are defined as the derivatives of the aerodynamic functions with respect to the design variables. In most cases, the main contributor to the optimization effort is the calculation of these derivatives; and, thus, it is desirable to have numerical methods that easily, efficiently, and accurately determine these coefficients for large complex problems. At present,[1–8] there are two primary approaches for calculating transonic aerodynamic sensitivity derivatives. In the first approach, the sensitivities are calculated by perturbing a design variable from its previous value, a new complete solution is obtained, and the differences between the new and the old solutions are used to obtain the sensitivity derivatives. This brute force direct technique is computer intensive for complex governing equations that include a large number of design variables. In the second approach, termed the quasianalytical (QA) method, the sensitivities are obtained by solving a large sparse system of algebraic sensitivity equations. While the matrix elements in these algebraic sensitivity equations are obtained analytically, they are obtained by analytically differentiating the discretized or numerical forms of the equations governing the flowfield. Furthermore, the aerodynamic and sensitivity solutions are obtained numerically. Thus, the method is termed a QA rather than a numerical or analytical method. It should be noted that the differentiations to obtain the coefficients for the algebraic sensitivity equations, while being straightforward in principle, are usually lengthy and tedious. However, once obtained, the sensitivity equations can be very efficient and accurate for computing large numbers of sensitivity coefficients.

In the first phase of this research[2] the QA approach was developed and applied to two-dimensional airfoils. Based upon these proof-of-concept investigations, it was concluded that the QA method was a feasible approach for accurately obtaining transonic aerodynamic sensitivity derivatives in two dimensions, and was often more accurate and efficient than the finite difference (FD) method as the number of design variables was increased. Furthermore, the algebraic forms of the matrix elements in the two-dimensional sensitivity equations were determined by hand, which involved extensive effort associated with differentiating the discretized residual with respect to the various design variables and the dependent unknowns. Today, such operations could be carried out using

Presented as Paper 92-2670 at the AIAA 10th Applied Aerodynamics Conference, Palo Alto, CA, June 22–24, 1992; received June 9, 1993; revision received Jan. 22, 1994; accepted for publication Jan. 22, 1994.

*Graduate Research Assistant; currently Assistant Professor, Cairo University, Egypt.
†Professor, Aerospace Engineering Department. Associate Fellow AIAA.

symbolic manipulation programs,[9] such as MACSYMA,[10,11] but present symbolic manipulators are incapable of automatically performing all the necessary simplification, combinations, and cancellations of terms associated with algorithmic simplification of expressions. Consequently, the user must be familiar with the commands available for the organization of expressions, and conduct various trials and experiments to identify a symbolic procedure that is efficient. As a result of these two-dimensional studies, it was decided to continue the research. Consequently, the primary objectives of the present effort have been to apply the QA method to three-dimensional transonic flow, investigate the use of symbolic manipulation programs[12,13] for obtaining the matrix elements of the sensitivity equations, and to determine the efficiency and accuracy of the QA approach for determining transonic aerodynamic sensitivities.

For this extended effort, it was decided to use for the flow solver a modified version of the three-dimensional direct-inverse analysis-design transonic full potential fully conservative code, ZEBRAII.[14-17] The full potential equation was selected because it can be solved rapidly and is robust and accurate for engineering purposes.[17] Also, it can be formulated using a stretched Cartesian grid system that can be rapidly generated and has simple metrics. Such a grid permits the variation of several design parameters without changing the physical or computational grids. For the present work, the analysis portions of ZEBRAII have been rearranged and unneeded portions deleted. In addition, the capability of calculating the sensitivity derivatives via the FD approach has been added.

Problem Statement

Application of the QA method to the full potential equation yields the sensitivity equation

$$\left(\frac{\partial R_{i,j,k}}{\partial \phi_{ii,jj,kk}}\right)\left(\frac{\partial \phi_{ii,jj,kk}}{\partial \boldsymbol{XD}}\right) = -\left(\frac{\partial R_{i,j,k}}{\partial \boldsymbol{XD}}\right) \tag{1}$$

where the residual expression in the computational plane in terms of backward differences is

$$R_{i,j,k} = \overline{\delta}_x(\tilde{\rho}U/J)_{i+1/2,j,k} + \overline{\delta}_y(\tilde{\rho}V/J)_{i,j,+1/2,k} + \overline{\delta}_z(\tilde{\rho}W/J)_{i,j,k,+1/2} \tag{2}$$

The retarded density coefficients in Eq. (2) are

$$\tilde{\rho}_{i+1/2,j,k} = (1 - \nu_{i+1/2,j,k})\rho_{i+1/2,j,k} + \nu_{i+1/2,j,k}\rho_{i-1/2,j,k} \tag{3}$$

$$\tilde{\rho}_{i,j+1/2,k} = \tfrac{1}{4}(\tilde{\rho}_{i+1/2,j,k} + \tilde{\rho}_{i+1/2,j+1,k} + \tilde{\rho}_{i-1/2,j,k} + \tilde{\rho}_{i-1/2,j+1,k}) \tag{4}$$

$$\tilde{\rho}_{i,j,k+1/2} = \tfrac{1}{4}(\tilde{\rho}_{i+1/2,j,k} + \tilde{\rho}_{i+1/2,j,k+1} + \tilde{\rho}_{i-1/2,j,k} + \tilde{\rho}_{i-1/2,j,k+1}) \tag{5}$$

where

$$\rho = \left[1 - \frac{\gamma - 1}{\gamma + 1}(U\Phi_X + V\Phi_Y + W\Phi_Z)\right]^{1/(\gamma-1)} \tag{6}$$

$$\nu = \min\left[1, \max\left(1 - \frac{M_c}{M^2}, 0\right)\right] \tag{7}$$

In Eq. (7), the Mach number is obtained from

$$\frac{1}{\rho} = \left(\frac{T_0}{T}\right)^{1/(\gamma-1)} = \left(1 + \frac{\gamma - 1}{2}M^2\right)^{1/(\gamma-1)} \tag{8}$$

and thus

$$M^2 = [2/(\gamma - 1)](\rho^{1-\gamma} - 1) \tag{9}$$

where ρ is nondimensionalized by ρ_0. From Eqs. (7) and (9)

$$\nu = \begin{cases} 0, & M < 1 \\ 1 - \dfrac{(\gamma - 1)M_c/2}{\rho^{1-\gamma} - 1}, & M > 1 \end{cases} \tag{10}$$

The contravariant velocities are

$$U = (X_x^2 + X_y^2)\Phi_x + X_y\Phi_Y \tag{11}$$

$$V = X_y\Phi_X + \Phi_Y \tag{12}$$

$$W = \Phi_Z \tag{13}$$

and the full potential is split into perturbation and freestream components as

$$\Phi_{i,j,k} = \phi_{i,j,k} + Xq_\infty \cos(\alpha) + Zq_\infty \sin(\alpha) \tag{14}$$

Note that the angle of attack enters the formulation through the above equation, and that the physical grid system (x, y, z) is transformed into the wing aligned computational grid (X, Y, Z) by

$$X(x, y) = \frac{x - xle(y)}{c(y)} \tag{15}$$

$$Y(y) = y \tag{16}$$

$$Z(z) = z \tag{17}$$

The boundary conditions are the surface boundary condition

$$W = U\frac{\partial z}{\partial X} + V\frac{\partial z}{\partial Y} \tag{18}$$

the Kutta condition along the wing semispan

$$\Gamma = \Delta\phi, \qquad x_{TE} < x \leq \infty \tag{19}$$

and the far-field boundary condition. Additional conditions include updating the potential on the downstream boundary ($\phi_x = 0$) and implementing the wing symmetry condition by setting $V = 0$.

Once the unknown sensitivities $\partial\phi/\partial\boldsymbol{XD}$ are obtained, the sensitivities of the pressure coefficient Cp with respect to the design variables can be computed. From the pressure coefficient expression

$$Cp = \frac{P - P_\infty}{\rho q_\infty^2/2} \tag{20}$$

substitution for the pressure using the isentropic relations yields

$$Cp = \frac{(\gamma + 1)/\gamma}{\rho q_\infty^2}(\rho^\gamma - \rho_\infty^\gamma) \tag{21}$$

where ρ is given by Eq. (6), and where the freestream values q_∞, ρ_∞, and P_∞ in Eqs. (20) and (21) are

$$q_\infty = \left(\frac{\gamma + 1}{\gamma - 1 + 2/M_\infty^2}\right)^{1/2} \tag{22}$$

$$\rho_\infty = \left(1 - \frac{\gamma - 1}{\gamma + 1}q_\infty^2\right)^{1/(\gamma-1)} \tag{23}$$

$$P_\infty = \frac{\gamma + 1}{2\gamma}\rho_\infty^\gamma \tag{24}$$

Design Variables

Design variables can be arbitrarily classified according to whether or not they are coupled. Uncoupled design variables are termed basic variables and are the independent variables that influence the solution of a problem. Coupled design variables are defined here to be nonbasic and are obtained from the basic design variables usually using simple algebraic expressions. For example, in the current problem, wing planform sweepback angles are defined as nonbasic design variables since they are obtainable from the basic variables, i.e., the coordinates of the corner points of the wing. Other examples of nonbasic design variables are the wing area, aspect ratio, and taper ratio.

The basic design variables for the current problem include freestream variables, airfoil cross-section variables, and planform parameters. The freestream design variables include M_∞ and α. The Mach number enters the formulations through Eq. (22), whereas the angle of attack shows up in Eq. (14). The airfoil section design variables include maximum thickness, maximum camber, location of maximum camber, and four angles that define at each spanwise station the amount of geometric twist. These variables enter the problem via the wing surface boundary condition, Eq. (18). The basic planform design variables define the geometry of the wing planform and are comprised of the coordinates of the wing corner points, which enter the formulation via Eq. (15). Evaluation of the sensitivities with respect to these basic planform variables allows the determination of the derivatives with respect to the nonbasic variables. Thus, for the current three-dimensional problem, the vector of design variables consists of 12 basic variables and is given by

$$\boldsymbol{XD} = (M_\infty, \alpha, T, C, L, T_1, T_2, T_3, T_4, XL_T, XT_T, Y_T) \tag{25}$$

These variables are used in obtaining the right-hand-side vectors in Eq. (1).

Note that the design variables listed in Eq. (25) form a complete set of the basic design variables influencing the aerodynamic solution for the wing planform and wing sections considered in the present investigation. If the wing planform were more complicated, having, e.g., a leading-edge break, then the coordinates of that break point would have to be included in the vector of design variables. For more complex configurations or for problems involving coupling such as aeroelastic phenomena, the design variable set would be found by examining the solution model(s) and determining which flowfield and geometric parameters appear and consequently affect the aerodynamic solution.

Symbolic and Numerical Treatment

The basic approach used to symbolically differentiate the residual expression was to treat the main expression in terms of smaller subexpressions, each of which was examined in terms of its constituents. This process was extended until the final subexpressions included the appropriate derivative argument, the reduced potential or the design variables, in a simple functional form. The best method to obtain these subexpressions was to consider the governing equation and the involved intermediate expressions in the original form given in Eqs. (2–14). This splitting or nesting of expressions with various intermediate dependencies declared in advance allowed each subexpression to be handled efficiently by the symbolic manipulator, in this case MACSYMA. This usage of the chain rule of differentiation together with the ability of the symbolic manipulator to keep track of various equations resulted in an efficient scheme of analytical differentiation. It is noted that an earlier attempt to obtain the derivatives from a residual expressed as an explicit function of reduced potential through appropriate substitutions—Eq. (14) into Eqs. (11–13) up to Eq. (2), proved to be a poor strategy since the rapid increase in expression size eventually caused the manipulator program to encounter limitations on memory and manipulative ability. The experience gained from this attempt, however, turned out to be useful in identifying the capabilities and limitations of various symbolic commands, and assisted in the development of further symbolic aspects associated with the project.

During this study, various symbolic manipulator codes were developed to assist in the application of the QA method. The first code, found all residual reduced potential dependencies. This code was needed prior to carrying out the analytical differentiation of the residual, Eq. (2), with respect to the reduced potential function. Notice that the latter function shows up in Eq. (14), where the details of the dependence of the residual expression on this function are not obvious, since intermediate expressions Eqs. (3–13) are involved. As mentioned earlier, handling each intermediate subexpression separately simplifies the operations involved. The result of this code was a file that included various intermediate dependencies obtained in the form of lists. The second code used these lists to perform the symbolic differentiation process to obtain the Jacobian and right hand side vectors for Eq. (1), and the result of this lengthy code was a large 15,000 line FORTRAN segment that included three subroutines. This segment is the heart of the QA method and is linked into the QA sensitivity driver. The third symbolic code generated FORTRAN source code for the derivatives of the pressure coefficient, Eqs. (21–25), with respect to the vector of design variables and used the reduced potential sensitivity derivatives as input arrays. This segment of FORTRAN source code was then also linked with the segment obtained from the second symbolic code. Finally, the fourth symbolic code was created during debugging operations to test the evaluation of various residual terms and was very helpful in revealing logic and procedure errors. Finally, it is important to emphasize that each of the above symbolic codes is executed only once followed by a transfer of the resulting source segments to the QA sensitivity driver. Details and sample MACSYMA codes for these processes are given in Ref. 4.

Direct solvers that were previously used in the two-dimensional problem[2] failed on the three-dimensional problem due to limitations on memory; whereas the iterative routines developed earlier worked properly but were very slow. However, library solvers[18] based on the iterative conjugate gradient (CG) method and the generalized minimum residual (GMRES) approach have been used with success and have proven to be extremely efficient with respect to memory and execution speed. For these solvers, the exact amount of storage needed depends on the sparsity and bandwidth of the Jacobian matrix, which in turn depends on the size of the three-dimensional grid. The present grid of $45 \times 30 \times 16$ yields a large, sparse, banded, and unsymmetric Jacobian matrix of $(43 \times 29 \times 14) \times (43 \times 29 \times 14)$ or about 17,500 $\times$ 17,500 that is less than 1% dense. An incomplete lower-upper (LU) factorization is applied only once to this large matrix, and the sensitivity equations are solved using the iterative CG or GMRES methods.[18–20] Following the factorization of the Jacobian matrix, back substitution using the known right-hand-side vectors generates the unknown sensitivity derivatives with a trivial computational cost. This approach exploits the efficiency of the QA method as the number of design variables is increased.

Program Structure

The analysis-sensitivity program consists of the modified flowfield analysis program, ZEBRA, the FD sensitivity driver, and the QA sensitivity driver. Execution of the main code starts with an analysis run followed by sensitivity derivative calculations carried out either using the FD method or the QA approach. The FD portion of code uses two consecutive

ZEBRA runs to calculate a vector of sensitivity derivatives. This brute force technique, while straightforward, has the disadvantage of being expensive to implement and exhibits problems when single precision variables are used. The QA driver consists of two main parts. The first part assembles the Jacobian matrix and the right-hand-side vectors through calls to the large code segment generated via symbolic manipulation. This section of subroutines, as explained earlier, contains source code for the elements of the Jacobian matrix and right-hand-side vectors. Following the numerical assembly step, the second part of the sensitivity driver solves the sensitivity equations using one of the available linear sparse solvers and yields the unknown sensitivity vectors at each point in the flowfield. Finally, the resulting sensitivity derivatives, $\partial\phi/\partial XD$, are processed to obtain the pressure coefficient sensitivity derivatives $\partial Cp/\partial XD$, at 25 chordwise locations at each of the 20 wing semispan stations.

Test Cases

For the present study, most of the test cases utilized the four cornered ONERA M6 wing planform[15-17] with a variety of airfoil sections including NACA 1406, 1706, 2406, and 2706 airfoils. This planform has an aspect ratio of 3.8 and a taper ratio of 0.56, with leading- and trailing-edge sweeps of 30 and 15.76 deg, respectively. Freestream conditions included subcritical cases at Mach 0.8 and an angle of attack of 1 deg, several supercritical transonic cases, and some supersonic cases up to Mach 1.2. Due to space limitations, most of the results of this article will be for the ONERA M6 planform with NACA 1406 airfoil sections at freestream conditions of Mach 0.84 and 3-deg angle of attack. This case is challenging since it has a subcritical lower surface flow and exhibits an upper surface shock wave located at 70% chord at the root that shifts to 10% chord at the tip and which increases in strength from the root to a point near the wingtip. Thus, the results for this case should be sufficient to demonstrate the capabilities of the present analysis-sensitivity method at transonic conditions. Complete detailed results for all the cases are presented in Refs. 4 and 21.

In the above cases, a coarse-medium grid sequencing was used in the flowfield computations to enhance convergence. For the FD method of computing the sensitivities, each design variable was individually perturbed a small amount, typically 1×10^{-6}, and a new flowfield solution obtained. In all cases, double precision arithmetic was utilized and the residual reduced eight orders of magnitude. In addition, the FD sensitivity results were computed by restarting each of the perturbed design states from the coarse grid, then proceeding to the medium grid. Different strategies for grid sequencing, such as starting on the medium grid with a previously obtained converged solution, are all valid options to speed up the FD approach; but these were not investigated in this study. In the QA method, the sensitivity equation, Eq. (1), was solved with 12 right-hand sides representing the vector of design variables, Eq. (25), using one of the sparse solvers. In all cases, $\partial\phi/\partial XD$ values were obtained for every gridpoint in the flowfield. Also, the method automatically computed upper and lower surface $\partial Cp/\partial XD$ values at 25 chordwise locations

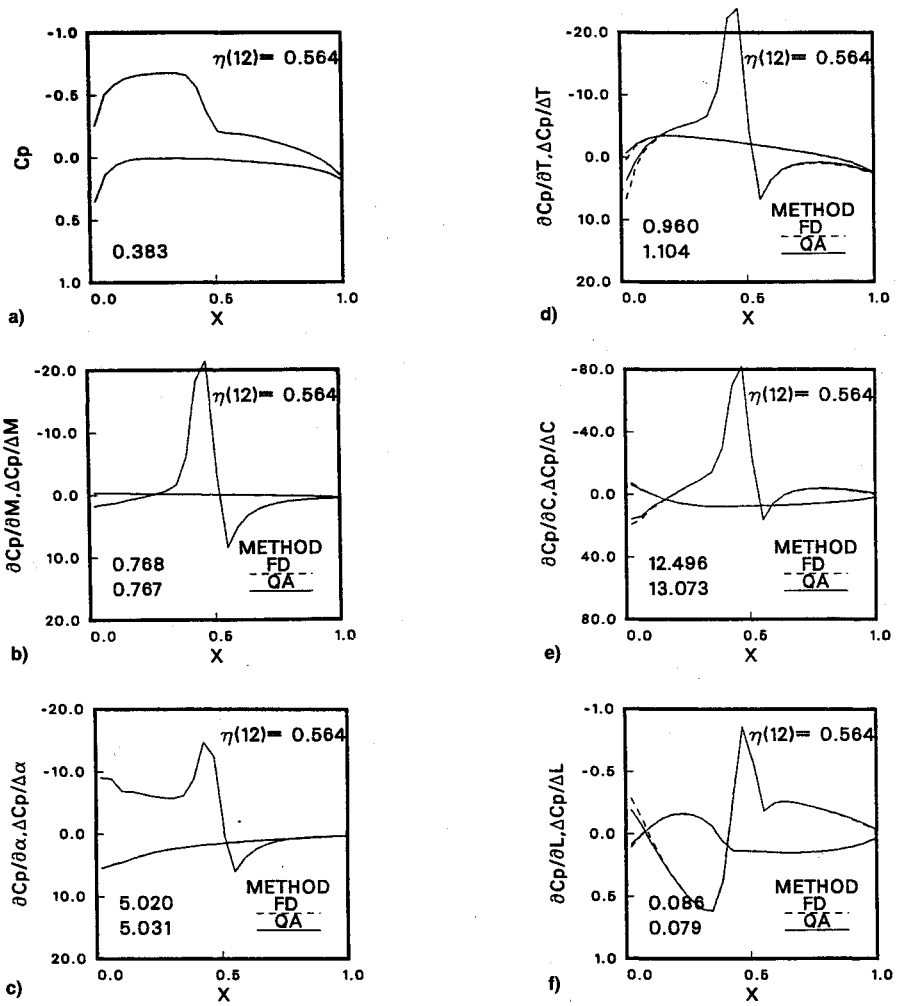

Fig. 1 Pressure coefficient and pressure coefficient sensitivity derivatives at 56% semispan, $M_\infty = 0.84$, $\alpha = 3$ deg. Values in lower left-hand corners are *Cl* for a). For b–f), they are the section $\partial CL/\partial XD_i$ computed by FD and QA methods: a) chordwise pressure coefficient, b) sensitivity to M_∞, c) sensitivity to angle of attack, d) sensitivity to thickness, e) sensitivity to camber, and f) sensitivity to camber location.

at each of the 20 semispan stations on the wing planform, as well as the $\partial Cl/\partial XD$ values at each of the span stations and the overall wing $\partial CL/\partial XD$ results.

Results and Discussion

For the subcritical test cases, the results obtained by the QA method were found to be in excellent agreement with results obtained from the FD method. In addition, the results followed the trend of the two-dimensional study.[2]

Representative results for the chordwise variation of the pressure coefficient and its sensitivity derivatives for a supercritical case ($M_\infty = 0.84$, $\alpha = 3$ deg) are shown on Fig. 1 for 56.4% semispan. Displayed in the corner in each case are the integrated coefficients, section lift coefficient for the pressure distribution, and $\partial Cl/\partial XD_i$ for the rest. In subcritical flow, the sensitivities with respect to the Mach number and the thickness would be small and similar for the upper and lower surfaces, while those for angle of attack, camber, and camber location would have larger upper and lower surface values of opposite sign. As expected, the sensitivity derivative profiles on Fig. 1 for the lower surface are typical of subcritical flow.[2] However, the upper surface results exhibit large variations in the vicinity of the shock wave that reflect the influence on the pressure of the sensitivity of the upper surface shock wave location to various design parameters. As can be seen by noting the differences in vertical scale, the pressures and lift coefficient at this mid-semi-span location are most sensitive to camber and least sensitive to camber location. Finally, the agreement between the FD and QA predictions is excellent, indicating that accurate three-dimensional transonic results can be obtained using the QA approach.

Some results for the spanwise variation of the section lift sensitivity derivatives are shown on Fig. 2, where the numbers in the lower left corner in this case are the total wing lift

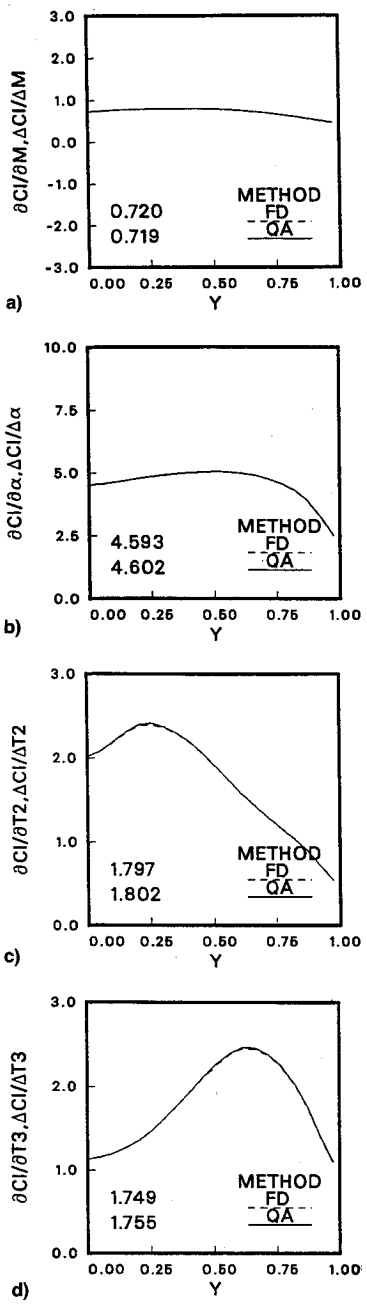

Fig. 2 Lift coefficient sensitivity derivatives, $M_\infty = 0.84$, $\alpha = 3$ deg. Values in lower left-hand corners are the wing $\partial CL/\partial XD_i$ computed by FD and QA methods: a) sensitivity to M_∞, b) sensitivity to angle of attack, c) sensitivity to twist at 20% semispan, and d) sensitivity to twist at 60% semispan.

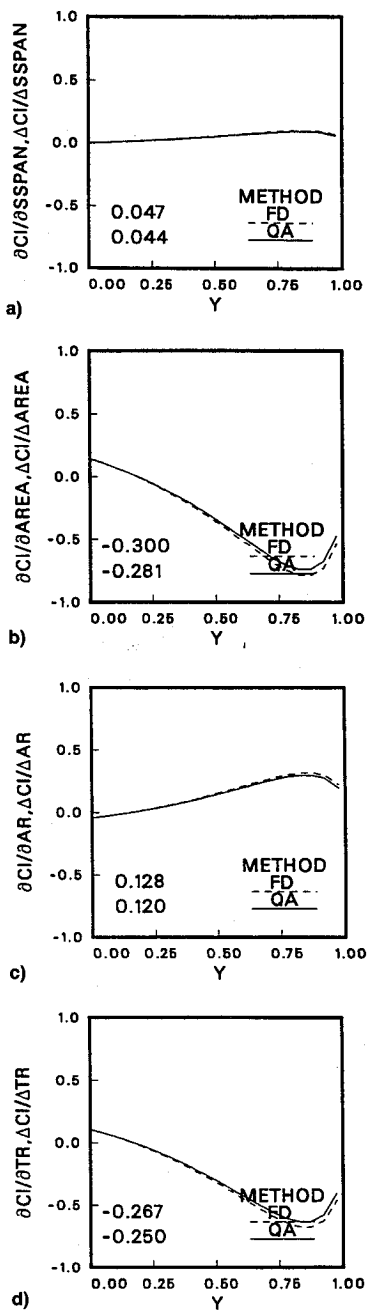

Fig. 3 Sensitivity to nonbasic design variables. Values in lower left-hand corners are the wing $\partial CL/\partial XD_i$ computed by FD and QA methods: a) sensitivity to semispan, b) sensitivity to wing area, c) sensitivity to aspect ratio, and d) sensitivity to taper ratio.

coefficient sensitivities, $\partial CL/\partial XD_i$. Note that the sensitivity of section lift to freestream Mach number and angle of attack is relatively constant over most of the semispan, but that the lift sensitivity to wing twist at 20 ($T2$) and 60 ($T3$)% semispan is concentrated in the region near the twist location. While not shown, lift sensitivities to twist at the root and the wingtip are only one-third to one-fourth of those at midspan. In general, primarily due to wing sweep and finite span, all the section sensitivity values are smaller in magnitude than corresponding values for the two-dimensional problem.[2] Finally, the agreement between the FD and QA section sensitivities is excellent.

Figure 3 shows representative section and wing lift sensitivity derivative results for some of the nonbasic design variables. While the total wing lift sensitivities can often be obtained by other means, the present method also yields spanwise and chordwise information. Note that while the lifts are relatively insensitive to the semispan, the outboard lift and total lift exhibit a strong dependence on area, aspect ratio, and taper ratio, and that the agreement between the QA method and the FD approach is reasonable. While not shown, the corresponding derivatives with respect to the leading- and trailing-edge sweep angles were very small.[4,21]

While both the FD and QA methods yield similar results, the present results indicate that for 12 design variables the QA method is about 2.4 times computationally more efficient than the brute force FD approach. However, it is recognized that the costs associated with the FD method probably could be reduced by executing the perturbed runs directly on the medium grid starting with the design point solution obtained from the coarse grid. Likewise, the QA method could be improved by utilizing various options associated with the sparse system equation solvers; and both methods are probably affected by grid size. Therefore, the stated relative efficiency should only be viewed as an estimate when comparing the two methods.

One application of sensitivity derivatives is solution prediction, and Fig. 4 compares two pressure coefficient distributions at the 56% semispan location predicted using a first-order Taylor series expansion about the original calculation point with the actual variation. The predicted Cp were calculated using

$$Cp_{\text{predicted}} = Cp_{\text{original}} + \left(\frac{\partial Cp}{\partial XD_i}\right) \Delta XD_i \qquad (26)$$

where the $\partial Cp/\partial XD_i$ values were obtained from the QA method at Mach 0.84 and $\alpha = 3$ deg. For the two results presented, the wing thickness was increased 8.3% to 0.065 chord, and the wingtip leading-edge ordinate was moved aft 0.1 chord, respectively. Since the original lift coefficient at this station, as shown on Fig. 1a, was 0.383, both changes resulted in a slight increase in lift coefficient and aft movement of the shockwave at this station. However, the detailed results[4,21] show that the movement of the wingtip ordinate caused a lift coefficient decrease in the inboard sections of the wing. As can be seen on the figure, the agreement between the quasianalytically predicted and actual pressure distributions is very good, which indicates that the sensitivity derivatives calculated using the QA method can be used for predictions. Similar results were obtained for the other design variables.[4]

Since sensitivity derivatives describe the response of the overall solution to changes in design variables, they can be computed over a range of flight conditions to determine the degree and nature of the influence of each design variable on the solution. At transonic conditions, the Mach number strongly influences a wing flowfield, and, thus, sensitivity derivatives were computed for the ONERA M6 planform with NACA 1406 cross sections at an angle of attack of 3 deg for Mach numbers ranging from 0.8 to 1.2. For simplicity, only the derivatives of the total wing lift coefficients with respect to

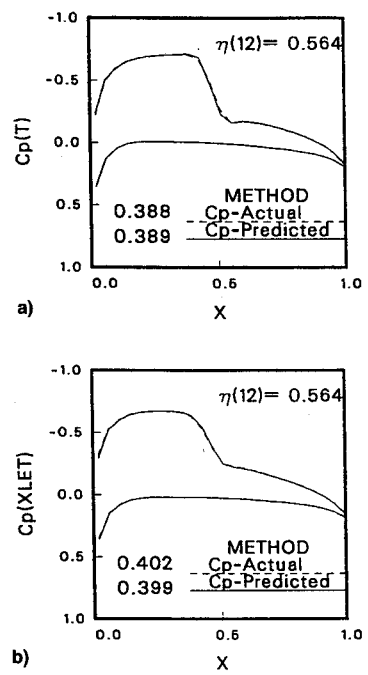

Fig. 4 Actual vs predicted pressure coefficients at 56% semispan. Values in lower left-hand corners are the actual and predicted section Cl: a) thickness increased to 0.065 chord and b) XL_T moved aft 0.1 root chord.

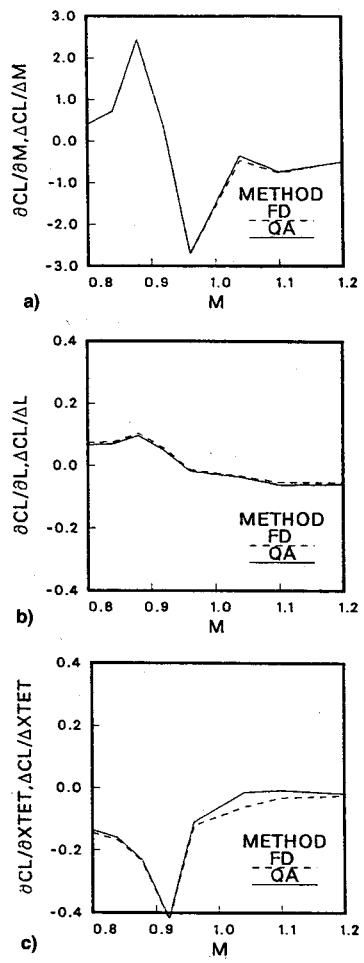

Fig. 5 Sensitivity of CL for $0.8 < M_\infty < 1.2$: a) sensitivity to M_∞, b) sensitivity to camber location, and c) sensitivity to wingtip trailing-edge ordinate.

each of the 12 basic design variables were considered. Figure 5 shows results for three of these design variables, freestream Mach number, maximum camber location, and wingtip trailing-edge ordinate. For all the design variables the largest variation of each derivative occurs in the transonic regime below Mach 1. In this range as Mach number increases, the upper surface shock wave is rapidly moving towards the trailing edge with the inboard portions reaching the trailing edge first. Thus, as shown by $\partial CL/\partial M_\infty$, there initially is an increase in wing lift coefficient. However, by Mach 0.92, the inboard portion of the shock wave is at or near the trailing edge, and the effects of lower surface pressure changes due to freestream Mach number increase cannot be compensated by aft shock wave movement, thus resulting in a less rapid (smaller derivative value of $\partial CL/\partial M_\infty$) rise in lift. By Mach 0.96 the entire upper surface shock wave is essentially at the trailing edge and the lift decreases, as indicated by the negative value of $\partial CL/\partial M_\infty$. As can be seen on the figure, the effects of this shock wave movement are captured by the variations in the sensitivity derivatives. Also, notice in Fig. 5 that for supersonic freestream Mach numbers the sensitivities are considerably lower. Additional results[4,21] show that the derivatives of the total lift coefficient exhibit their largest change with respect to M_∞, T, C, α, XL_T, XT_T followed by T_2, T_3, L, Y_T, T_4, and T_1, indicating that a hierarchy of dominance exists among the design variables for the current wing configuration. Finally, again there is good agreement between the results obtained by the QA method and the FD approach.

Conclusions

Based upon the above results, it is concluded that the QA method is a feasible and efficient approach for accurately obtaining transonic aerodynamic sensitivity coefficients in three dimensions. In addition, use of the symbolic manipulation packages to carry out the symbolic evaluation of the elements of the sensitivity equations is crucial in this type of sensitivity study. The results obtained from the QA method are almost identical to those obtained by the FD approach. Furthermore, the study indicates the following:

1) Obtaining the sensitivity derivatives using the QA approach and an iterative conjugate gradient method appears to be more efficient than computing the derivatives by the FD method, especially when the number of design variables is large.

2) The QA method shows promise with regard to analysis-sensitivity methodologies applied to large aerodynamic systems.

Acknowledgments

This project was supported by NASA under Grant NAG 1-793. Technical monitors were E. Carson Yates Jr. and Woodrow Whitlow Jr., NASA Langley Research Center. The authors also appreciate the helpful suggestions and discussions of Perry Newman of NASA Langley.

References

[1]Sobieski, J. S., "The Case for Aerodynamic Sensitivity Analysis," *Proceedings of the Symposium on Sensitivity Analysis in Engineering*, edited by H. A. Adelman and R. T. Haftka, NASA Langley Research Center, Hampton, VA, 1986, 1987, pp. 77–97 (NASA CP-2457).

[2]El-banna, H. M., and Carlson, L. A., "Determination of Aerodynamic Sensitivity Coefficients Based on the Transonic Small Perturbation Formulation," *Journal of Aircraft*, Vol. 27, No. 6, 1990, pp. 507–515.

[3]El-banna, H. M., and Carlson, L. A., "Determination of Aerodynamic Sensitivity Coefficients Based on the Three-Dimensional Full Potential Equation," AIAA Paper 92-2670, June 1992.

[4]El-banna, H. M., "Aerodynamic Sensitivity Analysis in the Transonic Regime," Ph.D. Dissertation, Texas A&M Univ., College Station, TX, Aug. 1992.

[5]Baysal, O., and Eleshaky, M. E., "Aerodynamic Design Optimization Using Sensitivity Analysis and Computational Fluid Dynamics," *AIAA Journal*, Vol. 30, No. 3, 1992, pp. 718–725.

[6]Dulikravich, G. S., "Aerodynamic Shape Design and Optimization," AIAA Paper 91-0476, Jan. 1991.

[7]Taylor, A. C., III, Korivi, V. M., and Hou, G. W., "Approximate Analysis and Sensitivity Analysis Methods for Viscous Flow Involving Variation of Geometric Shape," *Proceedings of the AIAA 10th Computational Fluid Dynamics Conference*, AIAA, Washington, DC, 1991, pp. 456–475 (AIAA Paper 91-1569).

[8]Baysal, O., Eleshaky, M. E., and Burgreen, G. W., "Aerodynamic Shape Optimization Using Sensitivity Analysis on Third-Order Euler Equations," *Journal of Aircraft*, Vol. 30, No. 6, 1993, pp. 953–961.

[9]Bau, H. H., "Symbolic Computation—An Introduction for the Uninitiated," *Symbolic Computation in Fluid Mechanics and Heat Transfer*, American Society of Mechanical Engineers, Vol. 97, 1988, pp. 1–10.

[10]*MACSYMA Reference Manual*, Version 13, Computer Aided Mathematics Group, Symbolics, Inc., Burlington, MA, 1988.

[11]*MACSYMA User's Guide*, Computer Aided Mathematics Group, Symbolics, Inc., Burlington, MA, 1988.

[12]Roach, P., and Steinberg, S., "Symbolic Manipulation and Computational Fluid Dynamics," *AIAA Journal*, Vol. 22, No. 10, 1984, pp. 1390–1394.

[13]Steinberg, S., and Roach, P., "Automatic Generation of Finite Difference Code," *Symbolic Computation in Fluid Mechanics and Heat Transfer*, American Society of Mechanical Engineers, Vol. 97, 1988, pp. 81–86.

[14]South, J. C., Jr., Keller, J. D., and Hafez, M. M., "Vector Processor Algorithms for Transonic Flow Calculations," *AIAA Journal*, Vol. 18, No. 7, 1980, pp. 786–792.

[15]Weed, R. A., Anderson, W. K., and Carlson, L. A., "A Direct-Inverse Three-Dimensional Transonic Wing Design Method for Vector Computers," AIAA Paper 84-2156, Aug. 1984.

[16]Carlson, L. A., and Weed, R. A., "A Direct Inverse Transonic Wing Design Analysis Method with Viscous Interaction," AIAA Paper 85-4075, Oct. 1985.

[17]Carlson, L. A., and Weed, R. A., "A Direct Inverse Transonic Wing Design Analysis Method with Viscous Interaction," *Journal of Aircraft*, Vol. 23, No. 9, 1986, pp. 711–718.

[18]*Guide and Reference*, IBM Engineering and Scientific Subroutine Library, Release 3, IBM Corp., Rept. SC23-0184-3, Kingston, NY, 1990.

[19]Saad, Y., and Schultz, M. H., "GMRES: A Generalized Minimum Residual Algorithm for Solving Nonsymmetric Linear Systems," *Journal of Scientific and Statistical Computing*, Vol. 7, No. 3, 1986, pp. 856–869.

[20]Sonneweld, A., Wesseling, B., and DeZeeuv, C., "Multigrid and Conjugate Gradient Methods as Convergence Acceleration Techniques," *Multigrid Methods for Integral and Differential Equations*, edited by D. J. Paddon and M. Holstein, Oxford Univ. Press (Clarendon), Oxford, England, UK, 1985, pp. 117–167.

[21]El-Banna, H. M., and Carlson, L. A., "A Compendium of Transonic Aerodynamic Sensitivity Coefficient Data," Texas Engineering Experiment Station Rept. TAMRF 5802-92-03, College Station, TX, July 1992.